Venzin et al., J Biotechnol Biomater 2016, 6:2
DOI: 10.4172/2155-952X.1000233

Journal of Biotechnology & Biomaterials

Research Article Open Access

Biocompatibility of Pegylated Fibrinogen and Its Effect on Healing of Full-Thickness Skin Defects: A Preliminary Study in Rats

Venzin CM[1], Jacot V[1], Berdichevsky A[2], Karol AA[3], Seliktar D[2], von Rechenberg B[3,4] and Nuss KMR[3]*

[1]*Department of Small Animal Surgery, Vetsuisse Faculty, University of Zurich, Switzerland*
[2]*Faculty of Biomedical Engineering, Technion-Israel Institute of Technology, Haifa, Israel*
[3]*Musculoskeletal Research Unit (MSRU), Vetsuisse Faculty, University of Zurich, Switzerland*
[4]*Center of Applied Biotechnology and Molecular Medicine (CABMM), University of Zurich, Switzerland*

Abstract

Introduction: A synthetic polymer polyethylene glycol (PEG), was conjugated to fibrinogen as a three-dimensional and biodegradable skin wound dressing matrix. This PEG-fibrinogen (PEG-fib) was tested *in vivo* in a skin wound time course study for its biocompatibility and biodegradation, after being delivered into the wound by injection and polymerized *in situ* by photo-activation.

Materials and methods: The nature of the inflammatory response to the implanted material in acute, 8 mm diameter, full-thickness skin lesions in rats was histologically evaluated at 7 days (n=6) and 14 days (n=6). Six wounds per time point were left untreated as controls.

Results: After 14 days, wounds of both groups were healed by up to 78% contraction and 22% epithelialization. Immune cells such as foreign body giant cells, macrophages, plasma cells and lymphocytes were seen in the PEG-fib treated wounds at both time points, however in low numbers and similar to controls. The amount of immune cells dropped between day 7 and 14. Remnants of the gel were found at day 7 in two of the PEG-fib treated wounds, no PEG-fib were found after 14 days in any of the wounds. There was no difference in epithelialization between the two treatments at both time points.

Discussion: The histological evaluation showed good biocompatibility of the PEG-fib, such that a foreign body reaction to the implant could be ruled out. The amount of immune cells was in accordance to a normal reaction to an implanted resorbable biomaterial.

Conclusion: The PEG-fib hydrogel is fully biocompatible as a skin wound dressing. It provides initial moisture to the wound bed and is gradually resorbed and replaced by structured skin tissue. An attractive future perspective would be to prepopulate the PEG-fib hydrogel with cells (e.g. fibroblasts), or load it with growth factors or other soluble mediators to further promote healing of complicated skin wounds.

Keywords: Biocompatibility; Wound healing; PEG-fibrinogen hydrogel; *In vivo*; Rat

Introduction

Acute or chronic skin defects with tissue loss are very common. The challenges in dealing with these are the long healing times, excessive scar tissue formation and impaired skin function. The duration of open wound management can significantly contribute to patient morbidity and increased cost of treatment [1,2].

Adult skin wound healing takes place largely by repair rather than by regeneration [3]. There is evidence that the inflammation during wound healing is directly responsible for fibrosis and the extent of scar formation [4]. In contrast regenerative healing has a notable reduction of inflammatory cell activity compared to repair tissue [5]. During the wound healing process, dressings should maintain suitable wound moisture, prevent microbial microfilms, remove dead spaces and be permeable for moisture and oxygen [6]. Conventional passive and non-resorbable wound dressings may adhere to the wound surface and the need for their frequent changes traumatizes newly built tissue [7]. Different types of newly developed resorbable wound dressings have - to some extent - overcome these disadvantages. Ideally they give structural support for cell ingrowth, are fully biocompatible (non-toxic and non-immunogenic), resorbable and undergo biodegradation at the rate of new tissue formation [6-10].

Biocompatibility is defined as "the ability of a material to perform with an appropriate host response in a specific situation" [11]. Biocompatible implants do not form a fibrous layer or capsule around the implant after the early inflammatory response has subsided [12] and show low counts of specific immune cells like lymphocytes, plasma cells and foreign-body giant cells (FBGCs). However, certain numbers of macrophages and FBGCs are needed for material degradation [13].

Scaffolds for skin regeneration or repair can consist of biological or synthetic materials. Although they play mainly a structural role in the wound site, some scaffolds may also provide signal transduction for wound healing. Biological materials such as collagen or fibrin may provide bio-functional signals that can promote tissue regeneration [14], but are not stable enough to remain in the wound for the entire healing process. Furthermore, these materials are often hampered by large batch-to-batch variability and non-uniform *in situ* degradation [10,15]. In contrast synthetic polymers such as polyethylene glycol

***Corresponding author:** Nuss KMR, Center of Applied Biotechnology and Molecular Medicine (CABMM), University of Zurich, Switzerland, Tel: 0049 170 2807788; E-mail: katja.nuss@vetclinics.uzh.ch

Received June 05, 2016; **Accepted** June 21, 2016; **Published** June 28, 2016

Citation: Venzin CM, Jacot V, Berdichevsky A, Karol AA, Seliktar D, et al. (2016) Biocompatibility of Pegylated Fibrinogen and Its Effect on Healing of Full-Thickness Skin Defects: A Preliminary Study in Rats. J Biotechnol Biomater 6: 233. doi:10.4172/2155-952X.1000233

(PEG) are easily controlled in terms of their physical and degradation characteristics, but are completely lacking bioactivity and cell signaling domains [16]. These materials also resist cell adhesion [17].

As a skin wound dressing, the combination of the synthetic polymer PEG with fibrinogen [18,19] addresses drawbacks of biological materials that outweigh the effects on the benefits of synthetics. Fibrinogen can be conjugated with linear polyethylene glycol diacrylate (PEG-DA) to create a PEGylated fibrinogen hydrogel scaffold [20]; the process is called PEGylation.

The main advantage of PEGylated natural protein biomaterials [21-28] is their unique features. The synthetic PEG provides the biophysical and structural properties of the hydrogel. The fibrinogen directs the biological response based on biological cell signaling domains on the protein that are tissue repair specific [29]. These signals encourage migration, attachment and differentiation of endothelial cells and smooth muscle cells [21,30]. Additionally, the fibrinogen affords the scaffold proteolytic sensitivity for *in situ* biodegradation by cell activated protease activity [31]. It has been shown, that PEG-fibrinogen is degraded *in vivo* by surface erosion, with a remarkably low foreign body response [32,33].

Moreover, the high water content of the PEG-fibrinogen helps to establish a physiological extracellular environment that stimulates dermal tissue healing [8]. The material is non-toxic [22,29] and compatible with a number of different cell types [29]. The *in situ* hydrogel gelation allows a homogeneous integration with the wound and the gelation reaction can be carried out in the presence of a mild photoinitiator and long-wave ultraviolet light [21,34,35].

The physical characteristics and the degradation kinetics of the material, such as porosity, swelling, compliance, bulk density, and degradability can be adjusted to the individual needs of the application by altering the composition of the constituents [21]. Most of the structural properties of the PEG-fibrinogen hydrogel are defined by the synthetic PEG component [21]. Modifications to the hydrogel network structure are possible by changing the combination of the synthetic PEG and endogenous fibrinogen.

To date, PEG-fib has been successfully tested *in vitro* as a three-dimensional cell culture scaffold [21,25,27,31,36-39]. *In vivo*, PEG-fib has been applied in wounded bone [24], heart [40,41] and skeletal muscle [42] but has yet to be tested in a skin wound healing application. Using the PEG-fib as a primary resorbable wound dressing that mimics the provisional fibrin ECM and enables cell ingrowth may be a promising approach.

This preliminary comparative study aims to assess the suitability of PEG-fib as a three-dimensional skin repair matrix. Secondarily, we aim to assess the nature of the inflammatory response on the implanted material.

The hypotheses of this preliminary study were that i) the material accelerates wound closure compared to untreated control wounds and ii) the PEG-fib hydrogel is biocompatible and resorbable within the test period of 14 days.

Materials and Methods

Study design

A case control study in experimental animals was performed. Wounds of 8 mm diameter were created in the back of six rats. The rats were randomly assigned to the 7 or 14 days group. In every rat, two wounds were treated with the hydrogel and two left untreated. The allocation of the 24 wounds to the PEG-fib "hydrogel treatment" or "no treatment" resulted in 3 cranial and 3 caudal wounds for each treatment group and time point. After sacrifice the wounds were evaluated macroscopically and histologically.

Experimental animals

Six Sprague Dawley rats with a body weight of 168–180 g (mean 173.5 ± 5.28 g) and an age of 6 weeks were used. The survival times were 7 days (group 1, n=3) and 14 days (group 2, n=3) after surgery. The animals were held in groups of three in standard individually ventilated cages with access to standard rat food (M/R Haltung Extrudat, Provimi Kliba) and conditioned water (ProMinent) ad libitum. The animal study was conducted according to the Swiss law of animal protection and welfare and was permitted through the official Swiss authorities (permission # 150/2013).

PEG-DA synthesis and protein PEGylation

PEG-DA was prepared from linear PEG-OH (MW 10 kDa; Fluka, Buchs, Switzerland) and characterized according to protocols described elsewhere [21]. Briefly, acrylation of PEG-OH was carried out by reacting a dichloromethane (Aldrich, Sleeze, Germany) solution of PEGOH with acryloyl chloride (Merck, Darmstadt, Germany) and triethylamine (Fluka) at a molar ratio of 150% relative to the –OH groups. The final product was precipitated in diethyl ether and dried under vacuum for 48 h. The PEGylation of human fibrinogen (Tisseel, Baxter AG, Vienna, Austria,) was performed according to protocols described by Dikovsky et al. [22]. Briefly, tris (2-carboxyethyl) phosphine hydrochloride (TCEP HCl) (Sigma) was added to a 3.5 mg/ml solution of fibrinogen in 50 mM PBS with 8M urea (molar ratio 1.5:1 TCEP to fibrinogen cysteine). After dissolution, a solution of PEG-DA (280 mg/ml) in 50mM PBS and 8M urea was added and reacted overnight. The molar ratio of PEG to fibrinogen cysteins was 5:1 (linear PEG-DA, 6 and 10 kDa). The PEGylated protein was precipitated by adding 4 volumes of acetone (Frutarom, Haifa, Israel). The precipitate was re-dissolved at 10 mg/ml protein concentration in PBS containing 8M urea and dialyzed against 50 mM PBS.

The sterile PEG-fib products were characterized for total protein concentration using a Nanodrop2000 (Thermo Scientific, Waltham, Massachusetts, USA). The rheological properties and the degree of PEG substitution were evaluated based on previous studies [22,43].

Surgery and in-life phase

The animals were positioned in ventral recumbency in general anesthesia (Induction 20 mg/kg BW Ketamine hydrochloride subcutaneously (s.c.), maintenance Isofluran (Attane TM Isofluran, Provet Ag, Lyssach, Switzerland) 2.5 Vol%/0.7 l/min O_2 via facemask). A template was used to standardize the location and distance of the wounds. Four full-thickness excisional wounds (8 mm diameter, Figure 1) were created under aseptic conditions in the back of the rats using a biopsy punch (Biopsy Punch, Ø 8 mm, Stiefel Laboratories SRL, Milano, Italy). The hydrogel precursor solution, containing 4.7% (w/v) PEG-DA, 0.7% (w/v) PEG-fib and 0.1% (w/v) Irgacure®2959 photo-initiator (Ciba Specialty Chemicals, Basel, Switzerland) was applied to two randomly selected wounds of the four. The PEG-fib was cross-linked by 5 min exposure to long-wave UV light (λ=365 nm, I=5 mW/cm^2). The two untreated wounds served as control. A bandage (Urgocell lite (Urgo GmbH, Sulzbach, Germany) was applied covering all four wounds and fixed with Leukoplast (BSN Medical GmbH, Hamburg, Germany). In the 14-days survival group the bandage was changed after 7 days.

Buprenorphine (Temgesic®, Essex Chemie AG, Luzern, Switzerland) 0.075 mg/kg BW was applied s.c. immediately after surgery. This was repeated 3 times every 8 h and thereafter an oral dose of 0.6 mg/250 ml in drinking water was given for two days. The animals were monitored twice a day for clinical signs of pain or discomfort and the bandage was checked for functionality.

Tissue harvest and histology technique

After 7 or 14 days, respectively, the animals were euthanized by intracardial injection of 2 mL Pentobarbital (Esconarkon, Streuli Pharma Ag, Uznach, Switzerland) with the animals being unconscious in CO_2 anesthesia. The bandages were removed and pictures of the wounds were taken (Figures 2a and 2b). The skin squares, each containing one wound were excised and pin-fixed on a Styrofoam block (Figure 3). After fixation with 4% formaldehyde for 1 day, the samples were paraffin embedded and 3 µm cross-sections were obtained perpendicular to the skin surface in the center of each circular wound. The sections were stained with Haematoxilin-Eosin (H&E) for microscopic examination and wound area measurements. Immuno-histochemically the sections were prepared for assessment of the presence of myofibroblasts by the analysis of alpha-smooth muscle actin expression.

Evaluation

PEG-fib hydrogel-treated and untreated wounds were compared for macroscopic appearance of wounds including discharge, swelling, reddening using a customized score (0: none, 1: mild, 2: moderate, 3: severe discharge/swelling/reddening). This was evaluated by one of the authors (KN) in a blinded fashion. For histological assessments, the following aspects were compared: presence of a basal membrane, amount of immune cells, number of transected blood vessels, granulation tissue maturity, wound size, length of new epithelium formation, scar thickness, horizontal wound contraction, scar depression and alpha-SMA expression.

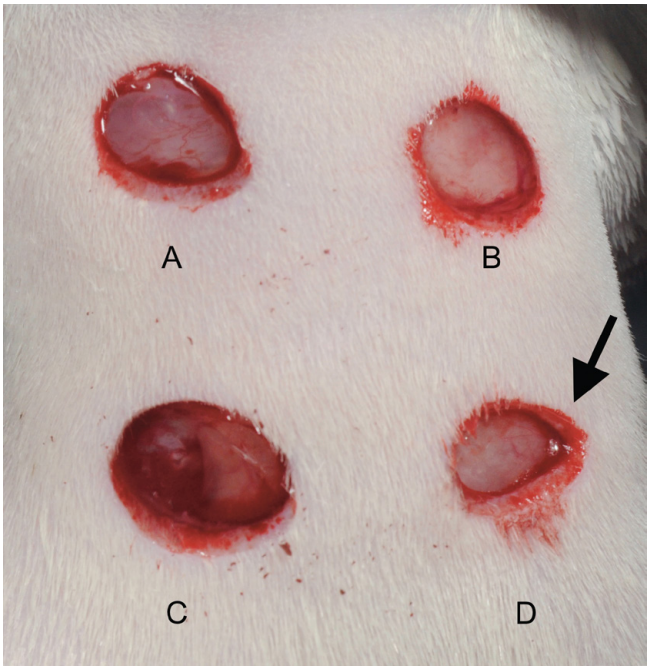

Figure 1: Surgery: Situation after punch biopsy of four full-thicknesses 8 mm diameter skin defects in a rat. PEG-fibrinogen hydrogel is already applied to wound A and C. Note the elliptical deformation of wound D according to skin tension (arrow).

Three observers with experience in wound healing histology (KN, VJ, AK) examined sections from each wound in a blinded fashion. The scores given by the three observers were averaged for each section. Qualitative wound healing parameters were obtained, such as the presence of a basal membrane as a sign for the restoration of an intact basement membrane zone connecting the epidermis and the underlying dermis.

The H&E stained sections were semi-quantitatively evaluated with a microscope (Leica MDL 505097, Leica Instruments GmbH, Nussloch, Germany) using a modified score [44,45] given in Table 1. The presence of immune cells (granulocytes, macrophages, lymphocytes, FBGCs) and material remnants was recorded as the mean of two non-overlapping high power optical fields (HPF) per section (20x magnification). One HPF was located at the periphery of the lesion, the other one in the middle (Figure 4). As a sign for the proliferative phase, the genesis of new capillaries was evaluated by the presence of preexisting vessels adjacent to the wound. Transected vessels were counted in one HPF within the granulation tissue at the center of the defect. Additionally, granulation tissue maturity was evaluated in terms of its principal cellular composition and the extent and regular arrangement of newly formed extracellular matrix.

The quantitative evaluation included several measurements (H&E stained histological sections) using the measurement tool of a specialized software program (Image access Standard 12, Glattbrugg, Switzerland). The evaluation was modified according to previously published methods [46,47] (see Figure 5).

The total wound area (TWA) was taken as the linear distance (µm) between wound and marginal tissue according to [47]. The open wound (OW) was taken as the length of the non-epithelized defect. The scar thickness at the defect center (STC) and at both wound margins (STM)

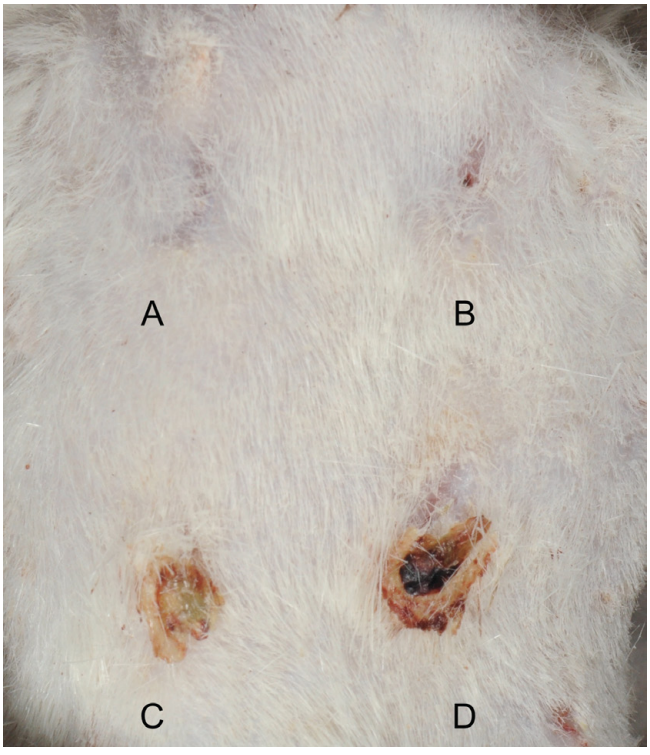

Figure 2a: Skin wounds 7 days post-surgery. A, D: Hydrogel-treated; B, C: Untreated controls.

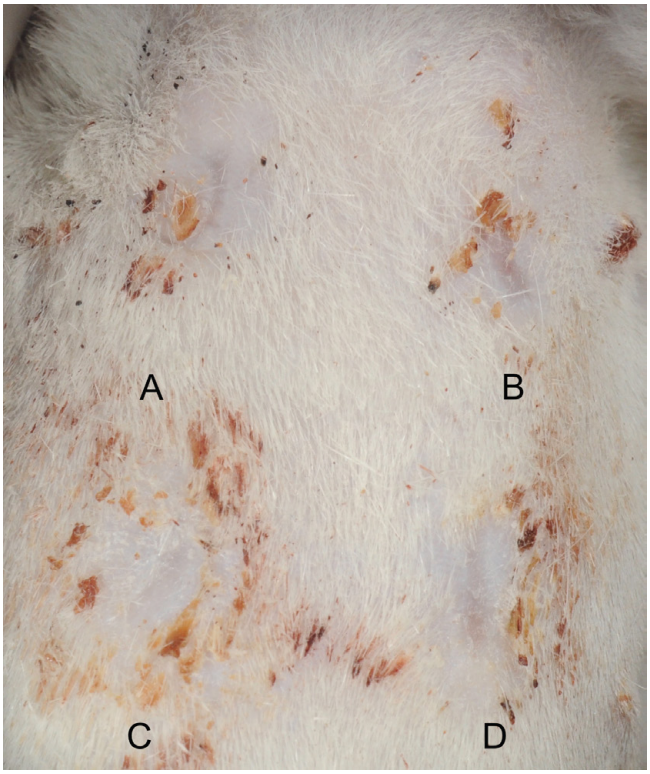

Figure 2b: Healed skin wounds 14 days post-surgery, A, D: Untreated; B, C: Hydrogel treated.

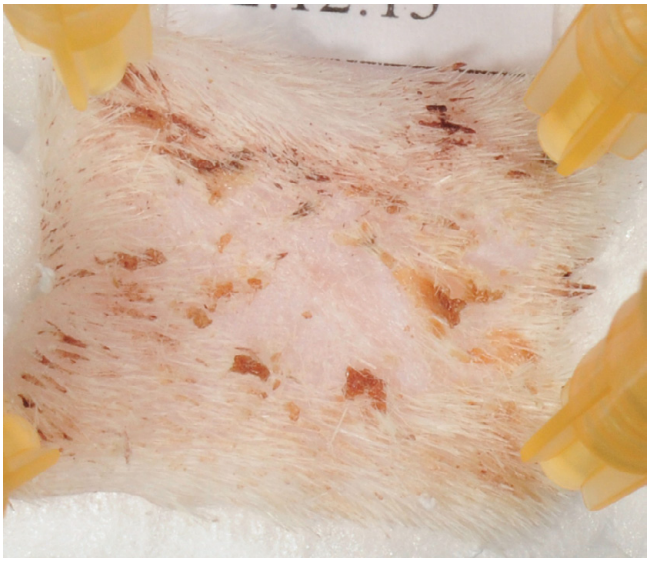

Figure 3: Pin-fixed skin sample before fixation (survival time 14 days, treatment: PEG-fibrinogen hydrogel).

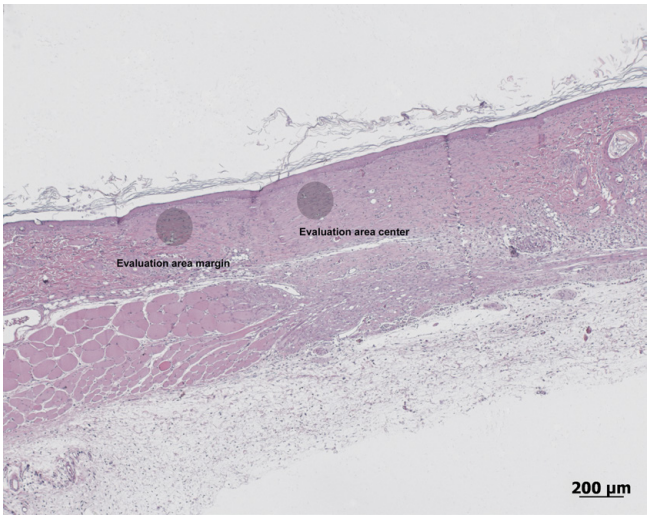

Figure 4: Histological section (14 days after surgery, staining: H&E) showing areas for evaluation of cell population, maturity of granulation tissue (periphery und center), and blood vessel cuts (center).

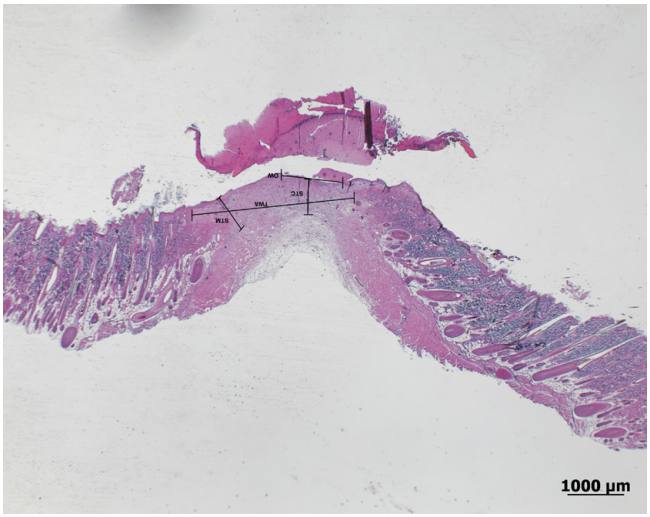

Figure 5: Histological section (7 days after surgery, staining: H&E) of wound area, illustrating measurements for:
TWA: Total Wound Area: Linear distance (µm) between wound and marginal tissue, open wound;
OW: Open Wound: Length of the non-epithelized defect;
STC: Scar Thickness at the defect center and at both wound margins (scar thickness margin: STM), measured from the top surface of the wound down to the panniculus carnosus.

was measured from the top surface of the wound down to the panniculus carnosus and taken as an indicator of the quantity of granulation tissue formed within the differently treated wounds [48].

Variables calculated

Horizontal contraction rate (HCR) was the defect size at surgery (8 mm) minus size of histological visible total wound area (TWA) in % taken as a measure of wound contraction. If no contraction had occurred, the wound width would be expected to remain at 8 mm, any reduction was considered to be wound contraction. Newly built epithelium (NBE) as a sign for the creation of a permeability barrier (re-epithelialization) was the TWA at sacrifice minus OW. The scar depression (VCR, vertical contraction rate) was the difference between scar thickness on wound margins (mean value of left and right margin) and center in %. The immunohistological stained sections were semi-quantitatively scored for the amount of alpha-SMA expression (Score see Table 1).

Statistics

Results were statistically evaluated using ANOVA, for the evaluation

of statistical significances the Bonferroni post-hoc test was performed. The level of significance was set as $p<0.05$.

Results

Surgery and in-life phase

Surgery and recovery from anesthesia were uneventful for all animals. The liquid hydrogel precursor solution was easily administered into the wound and polymerized within 5 min of UV light exposure. Upon cross-linking, the PEG-fib hydrogel precursor solution transitioned into a solid, elastic gel material that was not absorbed by the bandage. The bandages were well tolerated by the animals.

Macroscopical evaluation of wound healing

Macroscopically all wounds healed without complications and signs of unusual inflammation like reddening, swelling and severe discharge. After 7 days, most of the wounds showed a mild to moderate serous or sero-sanguinous discharge with no differences between treatments. After 14 days, a total of 6/12 wounds were completely healed, of which 5 were PEG-fib hydrogel treated and 1 was an untreated wound. The other wounds were evaluated as "in epithelialization", "almost closed" or with "very small defect". Otherwise no obvious differences between groups in wound or peri-wound appearance were detected.

Histological evaluation

Qualitative evaluation: A basal membrane was formed in most of the controls (controls: 5/6, PEG-fib 2/6) after 7 days and in all samples after 14 days (see Table 2). No fibrous layer was detected in any of the sections.

Semi-quantitative evaluation: The cell counts at the margin and in the center of the wounds, respectively, showed no significant differences between controls and treated wounds at both time points; an evaluation score of 2 was never exceeded. (Table 2). Significantly fewer granulocytes ($p=0.004$) and macrophages ($p=0.008$) were found in the middle of the wound after 14 days when comparing the 7 and 14 day results in the control group. This difference was smaller and not significant for the hydrogel group (Table 2).

No material remnants could be seen in all evaluated sections (both groups and time points) at the edge of the wound while in the middle of the wound up to 25% material remnants (Score 1) were found in 2 sections of the 7-days-group (Table 2) as an eosinophilic layer. This was not seen in the 14 days group. However, differences were not statistically significant ($p=0.221$).

After 7 days blood vessels were seen in treated and control wounds. The mean score for both the control and the hydrogel group was 3; after 14 days the score was reduced to 1 for both groups, with no significant

	Score 0	Score 1	Score 2	Score 3	Score 4
Cell counts	0 cells	1-10 cells	11-30 cells	31-60 cells	>60 cells
Blood vessels	0	1-5 vessel cuts	6-10 vessel cuts	>10 vessel cuts	-
Material remnants	0	<25%	25-50%	51-100%	-
Maturity of granulation tissue	Immature	Partially mature	Mostly mature	Completely mature	-
Basal membrane	Not present	Present	-	-	-
α-SMA expression	0	Low	Moderate	High	Very high

Table 1: Scores for evaluation of histological sections. The scores are based on the counts for immune cells (granulocytes, lymphocytes, macrophages, and foreign body giant cells), blood vessels, material remnants (percentage from original amount), maturity of granulation tissue, the presence of a basal membrane and alpha-SMA expression per optical high power field, 20x magnification.

	Survival time: 7 days		Survival time: 14 days		Comparison 7 and 14 days: p-value
	PEG-fib	Control	PEG-fib	Control	
Granulocytes edge	1.0 ± 0.63	1.33 ± 0.52	1.0 ± 0.63	0.5 ± 0.55	-
Granulocytes center	1.17 ± 0.41	1.5 ± 0.55*	0.67 ± 0.52	0.33 ± 0.52*	*0.004
Lymphocytes edge	1.67 ± 0.82	1.67 ± 0.82	1.0 ± 0.63	1.0 ± 0	-
Lymphocytes center	1.5 ± 0.55	2.0 ± 0.89	1.0 ± 0.63	1.0 ± 0.63	-
Macrophages edge	2.0 ± 1.27	1.83 ± 1.17	0.83 ± 0.98	0.5 ± 0.55	-
Macrophages center	1.5 ± 0.55	2.0 ± 0.63*	0.83 ± 0.75	0.67 ± 0.52*	*0.008
FBGC edge	0.17 ± 0.41	0.17 ± 0.41	0 ± 0	0 ± 0	-
FBGC center	0.17 ± 0.41	0.17 ± 0.41	0 ± 0	0 ± 0	-
Material remnants edge	0 ± 0	0 ± 0	0 ± 0	0 ± 0	-
Material remnants center	0.33 ± 0.52	0 ± 0	0 ± 0	0 ± 0	-
Blood vessels center	2.67 ± 0.52*[1]	2.67 ± 0.52*[2]	1.17 ± 0.41*[1]	1.17 ± 0.41*[2]	*[1]0.01 *[2]0.01
α-SMA expression	0.67 ± 0.82	1.0 ± 1.10	0.33 ± 0.82	0 ± 0	-
Maturity edge	1.67 ± 1.03	1.67 ± 0.82	2.33 ± 0.52	2.67 ± 0.52	-
Maturity center	1.33 ± 0.82*[1]	1.33 ± 0.52*[2]	2.67 ± 0.82*[1]	2.5 ± 0.55*[2]	*[1]0.019 *[2]0.049
Basal membrane	0.67 ± 0.52	0.83 ± 0.41	1 ± 0	1 ± 0	-

Table 2: Semi-quantitative and qualitative evaluation of histological sections, showing mean scores in the center or at the edge of the skin defect of: cell counts (Granulocytes, lymphocytes, macrophages, Foreign body Giant Cells (FBGC), material remnants, vessel counts, alpha-SMA expression, granulation tissue maturity and the presence of a basal membrane (n=12 wounds/time point). For the scores see Table 1. Differences between treated/untreated wounds were not significant; * indicates a significant difference between 7 day value and 14 days value, -: difference not significant.

differences comparing the treated and untreated wounds at both time points (Table 2). The reduction of vessel counts between day 7 and 14, however, was significant for both groups (p=0.001, see Table 2).

Comparison of granulation tissue maturity showed no significant differences between treated and untreated wounds at both time points. Comparison of maturation over time showed that the tissue matured significantly between day 7 and day 14 for the treated (p=0.019) and untreated (p=0.049, see Table 2) wounds.

Quantitative and calculated values: The mean diameter of the total wound area (TWA) was larger for the PEG-fib hydrogel treated wounds after 7 days (PEG-fib: 4085 μm, control: 3470 μm). This was reversed after 14 days (PEG-fib: 1792 μm, control: 2778 μm). Therefore, the reduction of total wound area over time was only significant for the PEG-fib hydrogel group (p=0.014), but not for the control group (Table 3).

A similar pattern was found for the diameter of the open wound (OW). After 7 days it was smaller in the untreated controls (1212 μm), as compared to the PEG-fib hydrogel treated wounds (2074 μm), but after 14 days this reversed to larger open wounds in untreated (404 μm) than in PEG-fib hydrogel treated wounds (no defect visible). The open wound diameter reduction over time was only significant for the PEG-fib hydrogel group (p=0.024) (Table 3).

The scar at the two histologically visible wound edges after 7 days was thicker for the hydrogel treated wounds (mean 1017 μm ± 126) than that of the untreated controls (808 μm ± 227). The reverse pattern was seen after 14 days (PEG-fib hydrogel: 592 μm ± 111, control: 608 μm ± 48). However, these differences between the treatments were not statistically significant at both time points (Table 3).

The measurement of the scar thickness in the middle of the wounds showed a similar pattern. After 7 days the scar was thicker for the hydrogel-treated wounds (1072 μm ± 300) than that of the untreated controls (719 μm ± 250). The reverse pattern was seen after 14 days (PEG-fib hydrogel: 543 μm ± 92, control: 663 μm ± 129). These differences between treatments at both time points were also not statistically significant. The calculated vertical compression of the scar was not significantly different between groups at either time points.

The mean horizontal contraction rate (%) in the 7-days group was calculated to be higher for the controls (56.61% ± 19.49) than for the PEG-fib hydrogel treated wounds (48.92 ± 12.23%). After 14 days this was reversed to a lower percentage for the controls (65.27% ± 15.14) than for the PEG-fib hydrogel treated ones (77.6 ± 7.72%) as shown in Table 3. These different values lead to a significant increase in wound contraction between day 7 and 14 for the PEG-fib hydrogel treated wounds (p=0.014, Table 3).

The calculation of newly built epithelium (NBE) showed no statistically significant differences comparing groups and time points (Table 3).

With regards to alpha-SMA expression, there were low levels expressed on day 7 (Figures 6a and 6b) in both groups, but no observable differences in the expression pattern after 14 days. There were no statistically significant differences in alpha-SMA expression levels between the treated and control groups at either time points (Table 2).

Discussion

Biomaterial scaffolds can provide distinct advantages in the treatment of difficult skin wounds; they can provide structural support and hydration to the wound bed, with additional versatility afforded through specific bioactivity at the material-cell interface [28].

In this preliminary study, the biocompatibility of a PEG-fib hydrogel applied in a skin defect in rats was evaluated, with a focus on the cellular reactions to the material, its resorption, and the subsequent formation of an epithelial layer in the topical application site.

The hydrogel was easily applied onto the wounds. The gel precursor solution spread out in the wound quickly and homogenously and integrated in the whole wound area; an advantage that has been reported accordingly [33]. After 5 minutes exposure to UV light, the hydrogel polymerized with consistency of elastic gels as previously reported [21]. This is highly advantageous, because the hydrogel may then maintain wound hydration until it is degraded and if necessary could be reapplied at bandage changes. The hydration could also have been achieved through bio-occlusive foils, but these devices have to be tailored to the wound geometry, because they cause irritations when covering healthy skin [49]. Furthermore, they may delay wound healing [49], have no absorption capability and may therefore accumulate exudates underneath, that would increase the risk of bacterial growth and reduce epithelialization [9].

Because both the test and control treatments were performed in the same animal, a cross contamination could not completely be precluded, but different to liquid substances the applied material was solid and fixed in the wound by the bandage, so that a transfer from one wound into the other seems unlikely.

A second intention healing by contraction and epithelialization occurred in all animals as would be expected in a healthy rodent non-adherent skin model. After 7 days, all wounds showed a sound granulation tissue and advanced epithelialization. After 14 days, 6 out of 12 wounds were closed macroscopically: 5 wounds treated with the

	Survival time - 7 days		Survival time - 14 days		Comparison 7 and 14 days: p-value
	PEG-fib	Control	PEG-fib	Control	
OW (μm)	2074.83 ± 1358.74*	1212.67 ± 1431.17	0 ±0*	404.00 ± 989.59	0.024
TWA (μm)	4085.83 ± 979.14*	3470.67 ±1559.92	1792.00 ±618.01*	2778.17 ± 1211.43	0.014
NBE (μm)	2011.00 ± 1363.48	2258.00 ±1383.93	1792 ±618.01	2374.17 ± 1289.42	-
HCR %	48.93 ± 12.24*	56.62 ± 19.50	77.60 ± 7.73*	65.27 ± 15.14	0.014
Scar thickness E (μm)	1017.08 ± 126.23*	808.42 ± 227.16	592.33 ± 111.81*	608.08 ± 48.61	0.001
Scar thickness C (μm)	1072.5 ± 300.53*	719.33 ± 250.36	543.83 ± 92.92*	663.5 ± 129.60	0.002
Scar vert. depr %	-4.25 ± 20.05	10.76 ± 22.50	7.16 ± 13.83	-9.50 ± 21.32	-

Table 3: Quantitative analysis of histological sections. The table summarizes the mean values (± standard deviation) for open wound at sacrifice (OW), total wound area (TWA), newly built epithelium (NBE), horizontal contraction rate percentage (HCR), scar thickness at edges (scar thickness E, mean of left and right edge), scar thickness in the center of the wound (scar thickness C), scar vertical depression (scar vert depr) percentage (difference between scar thickness at the edge of the wound and scar thickness in the center of the wound), *indicates a significant difference between 7 day value and 14 days value (n=12 wounds/timepoint), -: difference not significant.

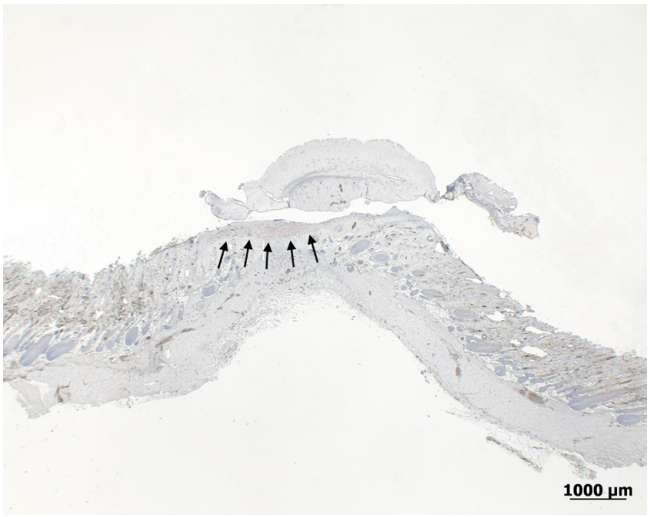

Figure 6a: Expression of alpha-SMA in granulation tissue of the healing wound 7 days after surgery (arrows).

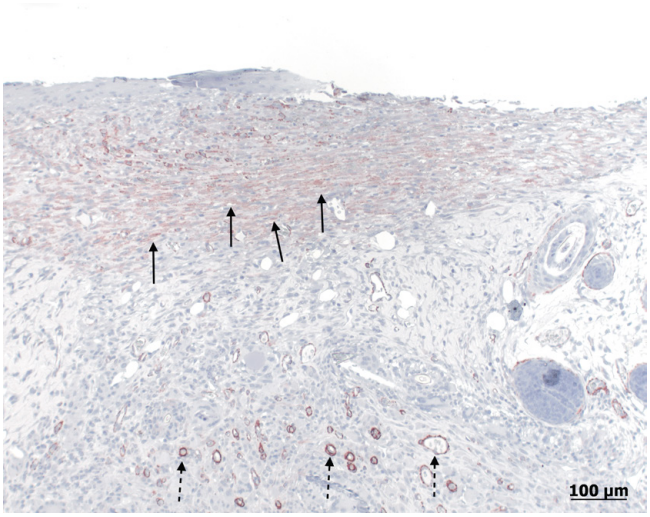

Figure 6b: Expression of alpha-SMA in granulation tissue of the healing wound 7 days after surgery (black arrows). Note that alpha-SMA is also expressed in different proportions in arterial walls by local smooth muscle cells (discontinuous arrows).

PEG-fibrinogen hydrogel and one of the untreated wounds. This is probably due to the effect of the hydrogel wound coverage, preserving a humid milieu throughout the treatment. It is generally accepted that maintaining a wet wound environment accelerates epithelialization [8,9]. It may also be a result of an interaction between the fibrinogen and inflammatory cells in the wound.

In our skin wound model the biomaterial showed good biocompatibility with no evidence of an unusual cellular reaction. This is in accordance with other in-vivo experiments where PEG-fib hydrogel biomaterials with progenitor cells were injected into the tibialis anterior muscle of mice [42]. It was shown that the PEG-fib hydrogels provided immediate protection from host inflammation for the implant progenitor cells. It also enhanced cell proliferation in acutely damaged and dystrophic muscles, leading to functional recovery of myofibers [42].

The cells detected in the histological sections of both groups at the two time points corresponded to the physiological cell repopulation in a healing skin defect. The short exposure to long-wave UV light radiation seems not to be cytotoxic to cells as it was already shown *in vitro* [39] and *in vivo* [42]. When comparing the untreated and hydrogel-treated wounds, there was no difference in the number of immune cells like FBGCs, macrophages, plasma cells and lymphocytes. Few of those cells, however, were seen in both groups as an indicator of an acute inflammatory reaction. Cell numbers in the hydrogel treated wounds may also be related to the higher load of material that requires breakdown by phagocytosis. Signs for incompatibility of the applied material such as high numbers of FBGCs in clusters, were not present. This is in accordance with findings of a study where the PEG-fibrinogen was implanted in subcutaneous pockets [32] in rats. Based on the prevailing evidence from these experimental observations, it can be stated that PEG-fib hydrogel is biocompatible for this intended application because no adverse consequences of the implanted material are evident, most notably no fibrous capsule was formed that might lead to unsatisfactory healing.

As for persistence of the PEG-fib hydrogel, remnants of the applied gel were found only in two of the treated wounds at the 7 days' time point, and no remnants were evident at the 14 days' time point. These findings are comparable to two *in vivo* rat studies, where PEG-fibrinogen was implanted in a subcutaneous pocket. The surface erosion of the bulk implant started at day 8 [32]. The model, where the hydrogel was polymerized *in situ*, showed a complete disassembly of the PEG-fibrinogen within 2 weeks, with an average of 90% material dissolved during the first week [33]. The rate of the PEG-fibrinogen degradation is highly dependent on the implantation site and the composition of the implant material. Previous studies demonstrated that the rate of biodegradation of the PEG-fib hydrogels could be affected both by the molecular weight of the grafted PEG, the molecular structure of the protein backbone [21] and the geometry of the implant [33]. Therefore, degradation kinetics can be changed in future studies using these material design parameters, if a longer persistence of the biomaterial in the wound is desired, e.g. in larger or deeper wounds.

The evaluation of the fibroblast maturity in the histological sections showed a partially mature tissue after 7 days, and almost completed tissue maturity after 14 days for both groups. There was a tendency for a higher tissue maturity of the PEG-fib hydrogel treated wounds after 14 days in the middle of the defect. This confirms previous results of *in vitro* studies with PEG-hydrogels [21,42]. Differentiation of newly built tissue is also supported by the fact that a basal membrane [50] was visible in all sections of the PEG-fib hydrogel treated and untreated control wounds at the 14 days' time point.

A significant reduction of blood vessels between day 7 and 14 was seen in the sections of both the control and the hydrogel treated groups. This reduction can be interpreted as a histological sign for uncomplicated healing, because prolonged vascularity is a sign of a scar that is likely to remain prominent [51]. In humans, the reduction of vessels does not begin until 2-3 weeks after the injury. The early reduction before day 14 can be most likely attributed to the rat model, where overall healing is faster than in most species, as shown by other authors [51].

After 7 days the amount of newly built tissue was greater in the untreated wounds, and therefore the open wound area was smaller for this group. However, after 14 days, all the PEG-fibrinogen-treated wounds were categorized as "closed" in the histological sections, while in the control wounds, an average open wound of 404 µm was still

observed. This was contrary to the macro-evaluation in one hydrogel-treated sample, were we saw signs for an open wound. Probably just a crust attached to the underlying healed epithelium lead to this misinterpretation [52]. When comparing the percentage of scar depression, it could be shown that after 7 days the treated wounds did not exhibit any scar depression in contrast to the untreated controls. After 14 days this difference was no longer evident. We speculate, that the positive results shown for the first week could be due to the structural support provided by the hydrogel, which allowed faster repair and subsequently faster remodeling between days 7 and 14. As a result, the thickness of the scar tissue was reduced.

Consequently, a wound contraction rate of 58% after 7 days and additionally 20% between 7 and 14 days was calculated. This rate is comparable to the data given in the literature where 50-90% wound contraction was seen in excisional wound in rats, depending on wound geometry, anatomical location and the presence or absence of panniculus carnosus [53,54]. There are models to limit wound contraction to a degree comparable to that of humans (25-40% [55]), including splints secured to the skin with adhesives [56]. However, splinting has been shown to alter wound healing, probably by mechanical and biochemical signaling in the wound, and it is not yet clear, whether the healing process induced by these models is actually closer to that of humans [57]. Because wound contraction is a direct result of myofibroblasts producing α–smooth muscle actin (alpha-SMA) [58], it was interesting to note, that low amounts of alpha-SMA were evident in the sections after 7 days. Likewise no more alpha-SMA could be detected at day 14. Although no myofibroblasts were visible at 14 days' time point, the contraction of the wound proceeded at the later time point, albeit to a much lesser degree. It is possible that histological methods were not sensitive enough, but it is also apparent that the myofibroblasts is not the only cell that generates contractile forces within wounds [58,59]. The significant drop of visible alpha-SMA over time is a sign for normal wound healing, where the myofibroblasts progressively disappear in the scar [60].

This study also has some limitations. First, the rat was chosen as the experimental animal model. On the one hand clinical observations generally indicate that wound healing follows the same basic pattern in most species and therefore a relatively homogenous process across species lines is assumed [47]. On the other hand, healing of rat wounds does not perfectly mimic the situation in full-thickness wounds of humans, because the skin morphology is somewhat different [54]. In addition, the wound contraction rate in rodents is higher [52] and the healing process is accelerated due to their faster overall metabolism [53]. Compared to the complexity of human chronic wounds the rodent model is relatively simple. However, the use of rodent models is fairly representative of acute wound healing in humans and accepted to test biocompatibility issues of novel biomaterials [61].

A second limitation of the study is the location of wounds. Wound location is highly relevant, because the wound contraction rate is variable in how tightly the skin is adherent to the underlying tissue [54]. Although location and the skin punch technique were standardized, the resulting size and shape varied to a certain extent. This is due to the remaining skin's elastic forces [62], which may deform the circular defect into an ellipse. The randomization of treatments can compensate for this effect, while higher animal numbers would equalize the differences. However, this preliminary study with a relatively small number of animals served mainly for testing the biocompatibility of the PEG-fib hydrogel. A pivotal study with higher animal numbers and additional time points is planned to address the functionality of the PEG-fib hydrogel in comparison to standard controls and other hydrogel biomaterials.

The 8-mm defect model represents the healing of a relatively small, acute and non-infected wound, which usually heals without major problems in human patients. The need for new ways to treat larger wounds and chronic/infected wounds will require a different model [63,64]. Furthermore, different experimental animals will be required (e.g. pigs [64-66]) to be closer to the clinical situation of non-healing wounds in humans.

In conclusion, these findings indicate that the PEG-fib hydrogel is fully biocompatible in skin wounds (corroboration of hypothesis 2). The PEG-fib can be used as an *in situ* polymerizable biomaterial that gradually resorbs into the wound within a 2-week time frame. As a conductive biomaterial (non-functionalized), it did not accelerate wound healing (rejection of hypothesis 1). Future studies using the biocompatible PEG-fib hydrogel can be performed with prepopulated living skin cells (e.g. fibroblasts) and/or loaded with growth factors or other soluble mediators, in order to identify a repair strategy that may accelerate skin wound healing.

Acknowledgement

The authors acknowledge Prof. Dr. med. vet. Frederik J. van Sluijs, Dipl. ECVS, for his invaluable advice with the manuscript. The authors also acknowledge Ms. Aymone Lenisa for preparing excellent histological sections and Ms. Flora Nicholls for her help with anesthesia.

References

1. Powers JG, Higham C, Broussard K, Phillips TJ (2016) Wound healing and treating wounds: Chronic wound care and management. J Am Acad Dermatol 74: 607-625.
2. Eming SA, Martin P, Tomic-Canic M (2014) Wound repair and regeneration: Mechanisms, signaling, and translation. Sci Transl Med 6: 265sr6.
3. Reinke JM, Sorg H (2012) Wound repair and regeneration. Eur Surg Res 49: 35-43.
4. Eming SA, Krieg T, Davidson JM (2007) Inflammation in wound repair: Molecular and cellular mechanisms. J Invest Dermatol 127: 514-525.
5. Leung A, Crombleholme TM, Keswani SG (2012) Fetal wound healing: Implications for minimal scar formation. Curr Opin Pediatr 24: 371-378.
6. Seaman S (2002) Dressing selection in chronic wound management. J Am Podiatr Med Assoc 92: 24-33.
7. Wasiak J, Cleland H, Campbell F (2008) Dressings for superficial and partial thickness burns. Cochrane Database Syst Rev CD002106.
8. Winter GD (1963) Effect of air exposure and occlusion on experimental human skin wounds. Nature 200: 378-379.
9. Huang YC, Chu HW, Huang CC, Wu WC, Tsai JS (2015) Alkali-treated konjac glucomannan film as a novel wound dressing. Carbohydr Polym 117: 778-787.
10. Lee K, Rowely J, Eislet P, Moy E, Bouhadir K, et al. (2000) Controlling mechanical and swelling properties of alginate hydrogels independently by cross-linker type and cross-linking density. Macromolecules 33: 4291-4294.
11. Williams DF (2008) On the mechanisms of biocompatibility. Biomaterials 29: 2941-2953.
12. Jones JA, Dadsetan M, Collier TO, Ebert M, Stokes KS, et al. (2004) Macrophage behavior on surface-modified polyurethanes. J Biomater Sci Polym Ed 15: 567-584.
13. McBane JE, Sharifpoor S, Cai K, Labow RS, Santerre JP (2011) Biodegradation and *in vivo* biocompatibility of a degradable, polar/hydrophobic/ionic polyurethane for tissue engineering applications. Biomaterials 32: 6034-6044.
14. Hubbell JA (2003) Materials as morphogenetic guides in tissue engineering. Curr Opin Biotechnol 14: 551-558.
15. Bryant S, Arthur J, Anseth K (2005) Incorporation of tissue-specific molecules alters chondrocyte metabolism and gene expression in photo-cross-linked hydrogels. Acta Biomater 1: 243-252.
16. Appelman TP, Mizrahi J, Elisseeff JH, Seliktar D (2011) The influence of

biological motifs and dynamic mechanical stimulation in hydrogel scaffold systems on the phenotype of chondrocytes. Biomaterials 32: 1508-1516.

17. Roberts MJ, Bentley MD, Harris JM (2002) Chemistry for peptide and protein PEGylation. Adv Drug Deliv Rev 54: 459-476.
18. Leach J, Bivens K, Collins C, Schmidt C (2004) Development of photocrosslinkable hyaluronic acid-polyethylene glycol-peptide composite hydrogels for soft tissue engineering. J Biomed Mater Res A 70: 74-82.
19. Leach J, Schmidt C (2005) Characterization of protein release from photo-cross-linkable hyaluronic acid-polyethylene glycol hydrogel tissue engineering scaffolds. Biomaterials 26: 125-135.
20. Gonen-Wadmany M, Goldshmid R, Seliktar D (2011) Biological and mechanical implications of PEGylating proteins into hydrogel biomaterials. Biomaterials 32: 6025-6033.
21. Almany L, Seliktar D (2005) Biosynthetic hydrogel scaffolds made from fibrinogen and polyethylene glycol for 3D cell cultures. Biomaterials 26: 2467-2477.
22. Dikovsky D, Bianco-Peled H, Seliktar D (2006) The effect of structural alterations of PEG-fibrinogen hydrogel scaffolds on 3-D cellular morphology and cellular migration. Biomaterials 27: 1496-1506.
23. Gonen-Wadmany M, Oss-Ronen L, Seliktar D (2007) Protein–polymer conjugates for forming photopolymerizable biomimetic hydrogels for tissue engineering. Biomaterials 28: 3876-3886.
24. Peled E, Boss J, Bejar J, Zinman C, Seliktar D (2007) A novel poly(ethylene glycol)-fibrinogen hydrogel for tibial segmental defect repair in a rat model. J Biomed Mater Res A 80: 874-884.
25. Schmidt O, Mizrahi J, Elisseeff J, Seliktar D (2006) Immobilized fibrinogen in PEG hydrogels does not improve chondrocyte-mediated matrix deposition in response to mechanical stimulation. Biotechnol Bioeng 95: 1061-1069.
26. Nerem RM, Seliktar D (2001) Vascular tissue engineering. Annu Rev Biomed Eng 3: 225-243.
27. Shapira-Schweitzer K, Seliktar D (2007) Matrix stiffness affects spontaneous contraction of cardiomyocytes cultured within a PEGylated fibrinogen biomaterial. Acta Biomaterialia 3: 33-41.
28. Shachaf Y, Gonen-Wadmany M, Seliktar D (2010) The biocompatibility of PluronicF127 fibrinogen-based hydrogels. Biomaterials 31: 2836-2847.
29. Seliktar D (2005) Extracellular stimulation in tissue engineering. Ann N Y Acad Sci 1047: 386-394.
30. Frisman I, Seliktar D, Bianco-Peled H (2010) Nanostructuring of PEG-fibrinogen polymeric scaffolds. Acta Biomater 6: 2518-2524.
31. Saadi T, Nayshool O, Carmel J, Ariche A, Bramnik Z, et al. (2014) Cellularized biosynthetic micro-hydrogel polymers, for intravascular liver tissue regeneration therapy. Tissue Eng Part A 20: 2850-2859.
32. Berdichevski A, Shachaf Y, Wechsler R, Seliktar D (2015) Protein composition alters *in vivo* resorption of PEG-based hydrogels as monitored by contrast-enhanced MRI. Biomaterials 42: 1-10.
33. Berdichevski A, Simaan Yameen H, Dafni H, Neeman M, Seliktar D (2015) Using bimodal MRI/fluorescence imaging to identify host angiogenic response to implants. Proc Natl Acad Sci U S A 112: 5147-5152.
34. Elisseeff J, McIntosh W, Anseth K, Riley S, Ragan P, et al. (2000) Photoencapsulation of chondrocytes in poly(ethylene oxide)-based semi-interpenetrating networks. J Biomed Mater Res 51: 164-171.
35. Nguyen KT, West JL (2002) Photopolymerizable hydrogels for tissue engineering applications. Biomaterials 23: 4307-4314.
36. Shapira-Schweitzer K, Habib M, Gepstein L, Seliktar D (2009) A photopolymerizable hydrogel for 3-D culture of human embryonic stem cell-derived cardiomyocytes and rat neonatal cardiac cells. J Mol Cell Cardiol 46: 213-224.
37. Seliktar D, Zisch AH, Lutolf MP, Wrana JL, Hubbell JA (2004) MMP-2 sensitive, VEGF-bearing bioactive hydrogels for promotion of vascular healing. J Biomed Mater Res A 68: 704-716.
38. Seliktar D, Nerem RM, Galis ZS (2003) Mechanical strain-stimulated remodeling of tissue-engineered blood vessel constructs. Tissue Eng 9: 657-666.
39. Mironi-Harpaz I, Wang DY, Venkatraman S, Seliktar D (2012) Photopolymerization of cell-encapsulating hydrogels: Crosslinking efficiency versus cytotoxicity. Acta Biomater 8: 1838-1848.
40. Plotkin M, Vaibavi SR, Rufaihah AJ, Nithya V, Wang J, et al. (2014) The effect of matrix stiffness of injectable hydrogels on the preservation of cardiac function after a heart attack. Biomaterials 35: 1429-1438.
41. Rufaihah AJ, Vaibavi SR, Plotkin M, Shen J, Nithya V, et al. (2013) Enhanced infarct stabilization and neovascularization mediated by VEGF-loaded PEGylated fibrinogen hydrogel in a rodent myocardial infarction model. Biomaterials 34: 8195-8202.
42. Fuoco C, Salvatori ML, Biondo A, Shapira-Schweitzer K, Santoleri S, et al. (2012) Injectable polyethylene glycol-fibrinogen hydrogel adjuvant improves survival and differentiation of transplanted mesoangioblasts in acute and chronic skeletal-muscle degeneration. Skelet Muscle 2: 24.
43. Peled E, Boss J, Bejar J, Zinman C, Seliktar D (2007) A novel poly(ethylene glycol)-fibrinogen hydrogel for tibial segmental defect repair in a rat model. J Biomed Mater Res A 80: 874-884.
44. Lee YB, Park SM, Song EJ, Park JG, Cho KO, et al. (2014) Histology of a novel injectable filler (polymethylmethacrylate and cross-linked dextran in hydroxypropyl methylcellulose) in a rat model. J Cosmet Laser Ther 16: 191-196.
45. Ikarashi Y, Toyoda K, Ohsawa N, Uchima T, Tsuchiya T, et al. (1992) Comparative studies by cell culture and *in vivo* implantation test on the toxicity of natural rubber latex materials. J Biomed Mater Res 26: 339-356.
46. Hart J, Silcock D, Gunnigle S, Cullen B, Light ND, et al. (2002) The role of oxidized regenerated cellulose/collagen in wound repair: effects *in vitro* on fibroblast biology and *in vivo* in a model of compromised healing. Int J Biochem Cell Biol 34: 1557-1570.
47. Bohling MW, Henderson RA, Swaim SF, Kincaid SA, Wright JC (2004) Cutaneous wound healing in the cat: A macroscopic description and comparison with cutaneous wound healing in the dog. Vet Surg 33: 579-587.
48. Kim I, Mogford JE, Chao JD, Mustoe TA (2001) Wound epithelialization deficits in the transforming growth factor-alpha knockout mouse. Wound Repair Regen 9: 386-390.
49. Schunck M, Neumann C, Proksch E (2005) Artificial barrier repair in wounds by semi-occlusive foils reduced wound contraction and enhanced cell migration and re-epithelization in mouse skin. J Invest Dermatol 125: 1063-1071.
50. Martin P (1997) Wound healing--aiming for perfect skin regeneration. Science 276: 75-81.
51. Lokmic Z, Darby IA, Thompson EW, Mitchell GM (2006) Time course analysis of hypoxia, granulation tissue and blood vessel growth, and remodeling in healing rat cutaneous incisional primary intention wounds. Wound Repair Regen 14: 277-288.
52. Chen L, Mirza R, Kwon Y, et al. (2015) The murine excisional wound model: Contraction revisited. Wound Repair Regen 23: 874-877.
53. Cross SE, Naylor IL, Coleman RA, Teo TC (1995) An experimental model to investigate the dynamics of wound contraction. Br J Plast Surg 48: 189-197.
54. Dorsett-Martin WA (2004) Rat models of skin wound healing: A review. Wound Repair Regen 12: 591-599.
55. Yannas IV (2008) The relation between wound contraction, scar formation and regeneration. Scar J 1: 1-15.
56. Wang X, Ge J, Tredget EE, Wu Y (2013) The mouse excisional wound splinting model, including applications for stem cell transplantation. Nat Protoc 8: 302-309.
57. Davidson JM, Yu F, Opalenik SR (2013) Splinting strategies to overcome confounding wound contraction in experimental animal models. Adv Wound Care (New Rochelle) 2: 142-148.
58. Ibrahim MM, Chen L, Bond JE, Medina MA, Ren L, et al. (2015) Myofibroblasts contribute to but are not necessary for wound contraction. Lab Invest 95: 1429-1438.
59. Nedelec B, Ghahary A, Scott PG, Tredget EE (2000) Control of wound contraction. Basic and clinical features. Hand Clin 16: 289-302.
60. Desmoulière A (1995) Factors influencing myofibroblast differentiation during wound healing and fibrosis. Cell Biol Int 19: 471-476.

61. Frank S, Kämpfer H (2003) Excisional wound healing. An experimental approach. Methods Mol Med 78: 3-15.

62. Montandon D, D'andiran G, Gabbiani G (1977) The mechanism of wound contraction and epithelialization: clinical and experimental studies. Clin Plast Surg 4: 325-346.

63. Kanno E, Toriyabe S, Zhang L, Imai Y, Tachi M (2010) Biofilm formation on rat skin wounds by *Pseudomonas aeruginosa* carrying the green fluorescent protein gene. Exp Dermatol 19: 154-156.

64. Roy S, Biswas S, Khanna S, Gordillo G, Bergdall V, et al. (2009) Characterization of a preclinical model of chronic ischemic wound. Physiol Genomics 37: 211-224.

65. Middelkoop E, van den Bogaerdt AJ, Lamme EN, Hoekstra MJ, Brandsma K, et al. (2004) Porcine wound models for skin substitution and burn treatment. Biomaterials 25: 1559-1567.

66. Sabino F, Hermes O, Egli FE, Kockmann T, Schlage P, et al. (2015) *In vivo* assessment of protease dynamics in cutaneous wound healing by degradomics analysis of porcine wound exudates. Mol Cell Proteomics 14: 354-370.